Toward Better Wireload Models in the Presence of Obstacles*

Chung-Kuan Cheng†, Andrew B. Kahng†, Bao Liu† and Dirk Stroobandt‡

†CSE Department
UC San Diego
La Jolla, CA 92093
Tel: 858-534-6184
Fax: 858-534-7029
e-mail: {kuan, abk, bliu}@cs.ucsd.edu

‡ELIS Department
Ghent University
Gent, Belgium B-9000
Tel: +32-9-264-3401
Fax: +32-9-264-3594
e-mail: dstr@elis.rug.ac.be

Abstract— Efficient and accurate interconnect estimation is crucial to design convergence. With System-on-Chip design, IP blocks form routing obstacles that cannot be accounted for by existing *a priori* wirelength estimations. In this paper, we identify two distinct effects of obstacles on interconnection length: (i) changes due to the redistribution of interconnect terminals and (ii) detours that have to be made around the obstacles. Theoretical expressions of both effects for point-to-point nets with a single obstacle are derived and compared to experimental observations. We also experimentally assess these effects for multi-terminal interconnections and in the presence of multiple obstacles. We single out cases where the effects are additive, which suggests the use of lookup tables and *equivalent blockage* relations. Our results are applicable in chip planning tools, where they enable improved accounting for obstacles in a priori wirelength estimation schemes.

I. Introduction

In deep submicron design, the importance of estimating interconnect parameters such as delay, power, wirelength and routability increases; such estimates are part of the objectives of partitioning, placement and floorplanning tools. Also, the EDA flow is experiencing a trend of combining front end planning and physical implementation to help design convergence. In this process an efficient yet accurate predictor of interconnect parameters (resource usage, performance, etc.) is crucial. The efficiency and accuracy of front end planning tools depend on the performance of floorplanning, placement and partitioning tools, which in turn depend on that of the interconnect predictor.

RTL planning flows must constantly struggle with the chicken-egg conflict impasse (i) budgeting the path delays within blocks and between blocks, and (ii) finding a (good) placement of the blocks. Typically, this impasse is broken by using initial *wireload models*, i.e., statistically derived (or calibrated) estimates of routing lengths for given-sized nets placed in given-sized regions. These wireload models are certainly needed within blocks (since the blocks have not even been synthesized, let alone placed), and occasionally also between blocks (i.e., at the chip level); they are always needed at *some* point in the design flow. In this paper, we target a priori (pre-placement) and on-line (during placement) wirelength estimations.

Wirelength estimation was initiated by Landman and Russo's paper [1] on Rent's rule, and enriched by later models of Donath [2], Davis et al. [3] and Stroobandt et al. [6]. A review of recent progress is given in [5]. Apart from techniques that estimate average wire lengths or wirelength distributions, individual net wirelength estimators have also been studied. These techniques exploit individual net information such as the bounding box or number of terminals to yield more accurate estimations. Current industry tools use lookup tables of wirelength as a function of number of terminals [9].[1] The aspect ratio of the region or net bounding box is found to have a considerable effect on the expected wirelength for nets with few terminals [8].

All of these papers are based on regularly placed circuits such as gate arrays or standard cell designs, with the exception of [9] which considers a building block design methodology. With the trend toward IP-block-based System-on-Chip (SOC) design, it is more likely that the presence of macro cells as obstacles (e.g., memories or noise-sensitive mixed-signal/analog/RF blocks which do not allow over-the-cell routing) may significantly lengthen wires and cause congestion[2]. Thus routing obstacles make traditional wirelength estimations deviate from reality; such effects must be identified and counted by today's wirelength estimators to guarantee design convergence. However, to the best of our knowledge, no work to date has provided interconnect wirelength estimates in the presence of routing obstacles. In [9], routing obstacles are handled by dividing routing area into small bins, applying global routing over bins and using lookup tables for each bin.

In this paper, we distinguish between several effects of rectangular routing obstacles on individual wirelengths (see Fig. 1):

Definition 1 (Non-blocked wirelength) *The non-blocked wirelength $L_{nb}(n,P)$ of an n-terminal net (with terminal set P) is its (rectilinear) Steiner minimal length.*[3]

Definition 2 (Blocked wirelength) *The blocked wirelength $L_B(n,P)$ is the (rectilinear) Steiner minimal length of the same n-terminal net such that no part of the wire is routed inside any of the obstacles (see Fig. 1).*

In all sections of this paper, except for Section IV, we analyze the average (expected) wirelengths over a large number of n-terminal nets where the terminals are uniformly distributed within the routing region. We therefore define

Definition 3 (Intrinsic wirelength) *The (expected) intrinsic wirelength $\bar{L}_i(n)$ of an n-terminal net is the average non-blocked wirelength over all point sets of size n in the region.*

Definition 4 (Redistribution wirelength) *The (expected) redistribution wirelength $\bar{L}_R(n)$ is the average non-blocked wirelength over all point sets of size n in the region that lie outside the obstacles (because obstacles are forbidden areas for all terminals, changing the location of all terminal points). The* ***redistribution***

*This work was supported in part by the MARCO Gigascale Silicon Research Center and a grant from Cadence Design Systems, Inc..

[1] Also, global routing may be used as a constructive estimator. Indeed, proponents of global routing – notably Scheffer and Nequist [10] – have argued that interconnect estimation can only be performed constructively. This is in some sense a religious issue (e.g., contrast with Monterey Design emphasis on non-constructive prediction and estimation). We believe that the door is still open to development of strong *non-constructive, a priori* interconnect estimation methods.

[2] Other types of IP blocks permit only prescribed route-overs or otherwise have much less over-block routing resources than the normal empty areas of the layout region. They also create 'blockage' by raising the cost of the route-overs.

[3] The wire length could also be defined as the length of the minimum spanning tree or another length, depending on the actual router. A lookup table of Steiner minimum tree lengths is presented in [9] and extended in [8] for a rectangular area of arbitrary aspect ratio.

0-7803-6633-6/01/$10.00 ©2001 IEEE.

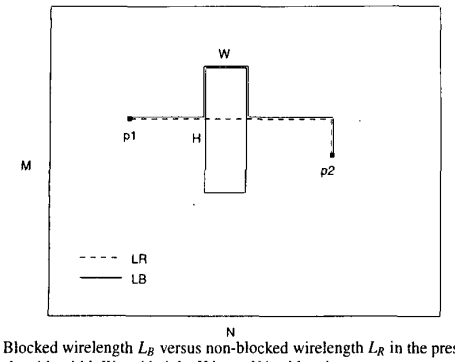

Fig. 1. Blocked wirelength L_B versus non-blocked wirelength L_R in the presence of an obstacle with width W and height H in an N by M region.

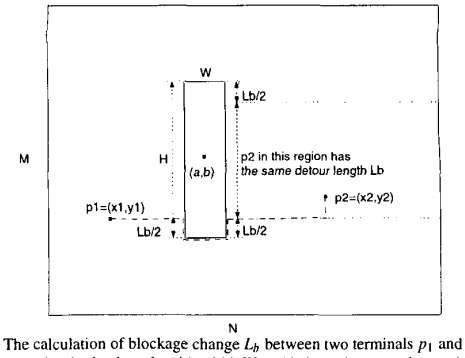

Fig. 2. The calculation of blockage change L_b between two terminals p_1 and p_2 in the presence of a single obstacle with width W and height H, centered at position (a,b).

change $\bar{L}_r(n)$ *(the change in wirelength due to redistribution) is given by*[4]

$$\bar{L}_r(n) = \bar{L}_R(n) - \bar{L}_i(n) \tag{1}$$

Definition 5 (Blockage wirelength) *The (expected) blockage wirelength $\bar{L}_B(n)$ is the average blocked wirelength over all point sets of size n in the region that lie outside the obstacles. The* ***blockage change*** $\bar{L}_b(n)$ *(the change in wirelength due to blockage) is then given by*

$$\bar{L}_b(n) = \bar{L}_B(n) - \bar{L}_R(n) \tag{2}$$

Several parameters influence the redistribution and blockage wirelengths in an SOC design: (i) the aspect ratio of the design itself, (ii) the number of net terminals, (iii) the number of obstacles, (iv) the area of obstacles, (v) aspect ratio of obstacles and (vi) locations of obstacles in the design. In the remainder of this paper, we separate these effects and make observations on their impact and significance with respect to wirelength distributions. Section II investigates designs with a single obstacle and study the influence of the dimension, aspect ratio and location of the obstacle, as well as the shape of the routing region. In Section III we extend our analysis to multiple obstacles. Section IV describes integration of our results in wirelength estimation models and Section V presents our conclusions.

II. Two-terminal Nets and a Single Obstacle

For this simple case, we are able to derive closed-form expressions for the effects of redistribution and blockage on the average wirelength. Experimental results verify these expressions.

A. Theoretical analysis

Under the assumption that all possible connections (all possible terminal pairs $(p_1 = (x_1, y_1), p_2 = (x_2, y_2))$) have an equal probability to occur, the average intrinsic wirelength of a two-terminal net in an N by M Manhattan grid can be calculated as

$$\bar{L}_i(2) = \frac{\int_0^N \int_0^N \int_0^M \int_0^M (|x_1 - x_2| + |y_1 - y_2|)\, dy_2\, dy_1\, dx_2\, dx_1}{\int_0^N \int_0^N \int_0^M \int_0^M dy_2\, dy_1\, dx_2\, dx_1} = \frac{N+M}{3} \tag{3}$$

Consider an obstacle with center at position (a,b), width W and height H. The average redistribution wirelength is found as the average Manhattan distance between net terminals p_1 and p_2 for all possible locations of p_1 and p_2 outside the rectangular area $(a - W/2 \le x \le a + W/2,\ b - H/2 \le y \le b + H/2)$ within the $N \times M$ region (Fig. 2). The result of the integration can be found to be [11]

$$\begin{aligned}\bar{L}_R(2) &= \frac{\int\int_A \int\int_A (|x_1 - x_2 + |y_1 - y_2|)\, dx_1\, dy_1\, dx_2\, dy_2}{\int\int_A \int\int_A dx_1\, dy_1\, dx_2\, dy_2} \\ &= \frac{1}{6\,(MN - WH)^2}\Big(2N^2M^2(N+M) + 2W^2H^2(H+W) \\ &\quad - 6NMHW(N+M-2(a+b)) - HW(MW^2 + NH^2) \\ &\quad - 12HW(Ma^2 + Nb^2)\Big).\end{aligned} \tag{4}$$

where A is the $N \times M$ region except the $W \times H$ obstacle. For a given region (given N, M), this equation is mainly dependent on the obstacle area WH, but there are also dependencies on W and H alone and on the location (a,b) of the obstacle center.

The blockage wirelength depends on the positions of the net terminals $p_1 = (x_1, y_1)$ and $p_2 = (x_2, y_2)$ relative to the obstacle. A detour because of the obstacle is only needed (see Fig. 2) if x_1 and x_2 (resp., y_1 and y_2) both are within $a - W/2$ and $a + W/2$ ($b - H/2$ and $b + H/2$) and if p_1 and p_2 are on opposite sites of the obstacle. Consider the case where p_1 is to the left of the obstacle (as in the figure) and assume that $y_1 < b$ (the other cases are similar). The vertical detour length is then found to be[5]

$$L_{bv} = \begin{cases} 2(y_2 - (b - H/2)) = 2y_2 + H - 2b & (b - H/2 \le y_2 \le y_1) \\ 2(y_1 - (b - H/2)) = 2y_1 + H - 2b & (y_1 \le y_2 \le b) \end{cases} \tag{5}$$

with a similar expression for the horizontal detour length L_{bh}. Taking care of all cases and using the symmetry in the problem, the average blockage change can be found to be [11]

$$\begin{aligned}\bar{L}_b(2) &= \frac{\int\int_A \int\int_A (L_{bh} + L_{bv})\, dx_1\, dy_1\, dx_2\, dy_2}{\int\int_A \int\int_A dx_1\, dy_1\, dx_2\, dy_2} \\ &= \frac{2}{3}\frac{H^3(N - a - \frac{W}{2})(a - \frac{W}{2}) + W^3(M - b - \frac{H}{2})(b - \frac{H}{2})}{(MN - WH)^2}\end{aligned} \tag{6}$$

where A is the $N \times M$ region except the $W \times H$ obstacle.

We see that the average blockage change is mainly dependent on the obstacle dimensions and more in particular the aspect ratio of the blockage. (Note that $a - W/2$ and $N - a - W/2$ are both large if W is small. Hence, a very tall and slim obstacle will result in a very large first term in Equation 6, and a negligible second term.) The blockage change is proportional to the third power of the largest dimension, hence it is superlinear in the largest obstacle dimension. From the equations, we have:

Observation 1 *The redistribution change mainly increases with the obstacle area.*

Observation 2 *The blockage change mainly increases with the largest obstacle dimension.*

[4] The redistribution change is solely due to the fact that terminals are relocated. Note that this can both increase and decrease the wirelength (consider, e.g., an obstacle in a corner). The redistribution change can therefore be negative.

[5] Also y_2 can be restricted to values smaller than b because of the symmetry.

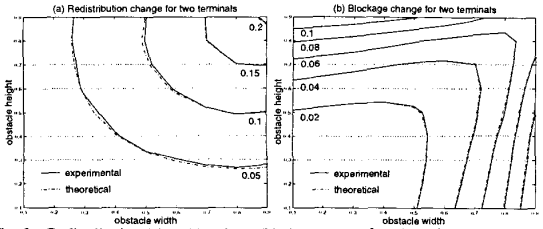

Fig. 3. Redistribution (a) and blockage (b) changes as a function of obstacle dimensions for two-terminal nets.

TABLE I
REDISTRIBUTION/INTRINSIC RATIO VS. DISPLACEMENT.

$dy\backslash dx$	0	0.05	0.1	0.15	0.2	0.25	0.3	0.35
0	1.0397	1.0417	1.0405	1.0342	1.0291	1.0223	1.0096	0.9994
0.05	1.0427	1.0406	1.0382	1.0352	1.0279	1.0226	1.0097	0.9990
0.1	1.0381	1.0381	1.0363	1.0313	1.0250	1.0178	1.0072	0.9952
0.15	1.0348	1.0331	1.0333	1.0268	1.0198	1.0121	1.0034	0.9930
0.2	1.0301	1.0276	1.0246	1.0192	1.0160	1.0064	0.9990	0.9843

TABLE II
BLOCKAGE/REDISTRIBUTION RATIO VS. DISPLACEMENT.

$dy\backslash dx$	0	0.05	0.1	0.15	0.2	0.25	0.3	0.35
0	1.0238	1.0238	1.0228	1.0209	1.0185	1.0150	1.0111	1.0063
0.05	1.0242	1.0233	1.0227	1.0212	1.0187	1.0153	1.0114	1.0065
0.1	1.0240	1.0238	1.0226	1.0208	1.0181	1.0152	1.0113	1.0065
0.15	1.0238	1.0234	1.0222	1.0207	1.0187	1.0153	1.0112	1.0062
0.2	1.0240	1.0238	1.0225	1.0209	1.0185	1.0148	1.0111	1.0059

B. Experimental observations

B.1 Experimental setup

To experimentally verify our theoretical analysis and extend our study to multi-terminal nets and multiple obstacles, we have developed a program to observe the redistribution and obstacle wirelengths. The program takes as inputs a set of obstacles and their dimensions and locations, as well as the number of net terminals. For calculation of the redistribution wirelength, obstacles are treated as areas where net terminals are not allowed but wires can pass through. For the calculation of the blockage wirelength, routing is is prohibited inside the obstacle areas. We use a unit square layout region unless we specifically investigate the influence of the shape of the region. Average values are obtained over uniformly random terminal sets (100,000 sets per run for all experiments).

For each random terminal set, a visibility graph is constructed wherein each terminal, each obstacle corner and each Hanan point (intersection of vertical and horizontal lines through each terminal and each obstacle corner) is a vertex. There is an edge for each pair of vertices for which the Euclidean straight line segment between the vertices does not intersect any other obstacle; this edge has weight equal to the Manhattan distance between the vertices. A rectilinear graph Steiner minimal tree heuristic [12] is then applied over this visibility graph to find the blocked wirelength.

B.2 Effect of obstacle dimensions

In a first experiment we study the effects of the obstacle's width and height on the redistribution and blockage wirelengths, for a single obstacle centered at (0.5,0.5) in a unit square region. Fig. 3(a) shows a contour plot of the redistribution change and Fig. 3(b) shows the contour plot of the blockage change as a function of obstacle dimensions. The plots also show the theoretical result superposed on the experimental observations. The curves match, as we expect.

Observations 1 and 2 are are supported, and for most obstacles, the redistribution effect is larger than the blockage effect (for square obstacles the ratio is about 2 to 1). Only for very high-aspect ratio shapes does the blockage effect exceed the redistribution effect.

B.3 Effect of obstacle location

In the previous experiment the obstacle was centered in a unit square region. Here, we study the effects of redistribution and blockage, as a function of the displacement (dx, dy) of the obstacle's center from the center of the unit square. To see the effects of displacement for oblong obstacles, we choose an obstacle with dimensions 0.2×0.5. Table I shows that the ratio of redistribution and intrinsic lengths decreases with larger displacements. The redistribution change even becomes negative (ratio < 1) for obstacles close to the region boundary. Table II shows a slightly different picture. Movements in the x-dimension result in a similar decrease in blockage effect (blockage wirelength over redistribution wirelength) but movements in the y-dimension (i.e., the dimension of the larger obstacle side) seem to have no effect at all.

Observation 3 *The closer the obstacle is to the boundary of the routing region, the smaller are the redistribution and blockage effects.*

Observation 4 *For very high-aspect ratio obstacles, displacements in the dimension of the longest obstacle side have no effect on the blockage change.*

B.4 Effect of the shape of the routing region

Another factor determining wirelength is the aspect ratio of the routing region. To study it, we keep an obstacle at the center of a routing region of unit area and change the region's aspect ratio. Again, we choose an oblong obstacle (with dimensions 0.1×0.2) to see the non-symmetrical effects. Fig. 4 shows the redistribution $(\bar{L}_R/\bar{L}_i)$, the blockage $(\bar{L}_B/\bar{L}_R)$ and the overall $(\bar{L}_B/\bar{L}_i)$ effects for variations of the aspect ratio $AR = N/M$ while the total area NM remains 1, both for theoretical equations and experimental results. For aspect ratios other than 1, the total wirelength increases. However, for a decreasing aspect ratio ($N < M$, i.e., region turns oblong in same way as obstacle), this is almost totally due to the redistribution effect alone. The blockage wirelength remains roughly the same. For increasing aspect ratios ($N > M$, i.e., region turns oblong in opposite way as obstacle), the inverse happens. The redistribution wirelength remains roughly the same but the blockage increases rapidly, dominating the rapid increase in total wirelength.

Observation 5 *When the aspect ratios of region and obstacle are similar, the redistribution effect dominates. When the aspect ratios are opposite, the blockage effect dominates. The latter case results in a longer wirelength, hence, it is better to line up obstacles with the region.*

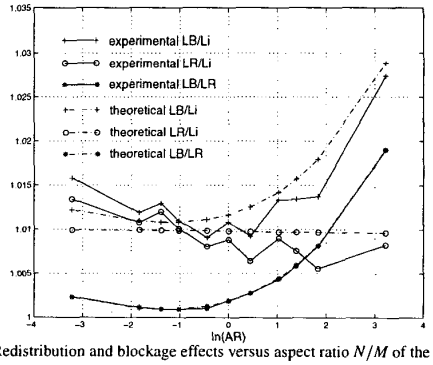

Fig. 4. Redistribution and blockage effects versus aspect ratio N/M of the region.

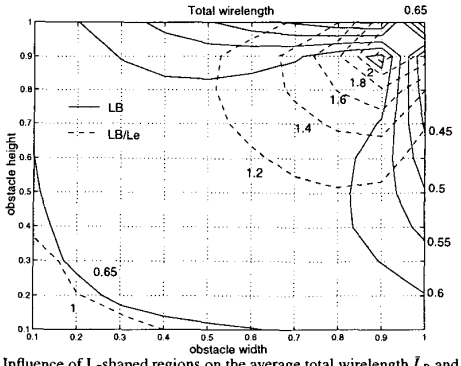

Fig. 5. Influence of L-shaped regions on the average total wirelength $\bar{L}_B$ and comparison to the wirelength $\bar{L}_e$ of an equivalent rectangular region with same area.

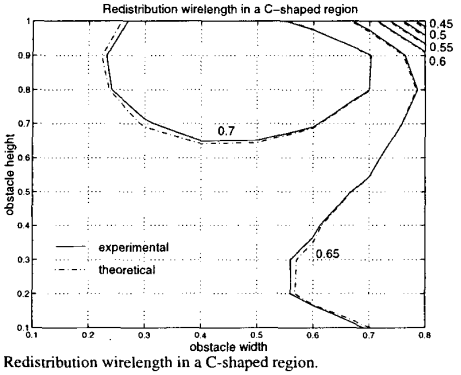

Fig. 6. Redistribution wirelength in a C-shaped region.

We also study the effect of an L-shaped region. For this, we keep an obstacle at a corner of the routing region and change its width and height. Fig. 5 shows the total wirelength that results for these experiments. It is always lower than the intrinsic wirelength (2/3) because (i) no wire is blocked (no terminals can be on opposite obstacle sites) and (ii) the amount of long wires "lost" because of redistribution is relatively higher than the amount of short wires "lost" thus decreasing the redistribution wirelength.[6] For increasing obstacle dimensions, the total wirelength decreases further and much more rapidly for oblong than for square obstacles.

The figure also shows the ratio of total (redistribution) wirelength versus the intrinsic wirelength $\bar{L}_e$ of an equivalent rectangular region with the same area as the L-shaped region. The more apparent the L-shape is (larger blockages in corner), the higher the discrepancy between its total wirelength and that of the equivalent rectangular region.

Observation 6 *Obstacles in the corner of the routing region (forming an L-shaped region) have a negative redistribution change and no blockage effect.*

Observation 7 *The more the L-shaped region deviates from a rectangle, the larger its total wirelength.*

We also have analyzed C-shaped routing regions, which are equivalent to obstacles touching the boundary of the rectangular routing region.[7] In this case the redistribution wirelength can still be expressed as Equation 4, while the blockage change doubles

[6]Consider an obstacle that occupies one quarter of the region. Half of the longest wires (diagonals) are lost, but only one quarter of the short wires (within a quadrant) are lost.

[7]In real routers, this includes the cases where there is still space between the obstacle and the routing region boundary but the space is not large enough to allow routing.

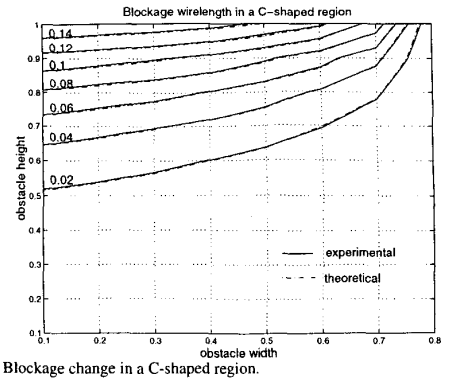

Fig. 7. Blockage change in a C-shaped region.

because half the wires that used one side of the obstacle for the detour now have to use the other (further) side [11]

$$\bar{L}_b(2) = \frac{4}{3}\frac{H^3(N-a-\frac{W}{2})(a-\frac{W}{2})+W^3(M-b-\frac{H}{2})(b-\frac{H}{2})}{(MN-WH)^2} \quad (7)$$

To verify the theoretical expressions, we use a $W \times H$ obstacle centered at $(0.5, 1-H/2)$. Figure 7 and Figure 6 show the contour plots of wirelengths as a function of obstacle dimensions. The theoretical and experimental plots are consistent and show that (i) the blockage change is larger for changes in the obstacle height (in the direction that touches the region boundary) than for changes in the obstacle width and (ii) the redistribution wirelength is a little larger than the intrinsic wirelength (2/3) except for very wide obstacles.

For multi-terminal nets we can obtain a theoretical analysis using similar techniques as for two-terminal nets and observe similar contour graphs of wirelength to obstacle dimensions [11]. This suggests to have a lookup table to characterize the obstacle impact on wirelength and leads to the following observation.

Observation 8 *For a larger number of terminals, both redistribution and blockage effects decrease. The redistribution effect is more sensitive to the number of terminals than the blockage effect.*

III. Multiple Obstacles

A. Theoretical analysis

For two-terminal nets, the average redistribution wirelength can be calculated for any number of obstacles as follows.

Consider m obstacles with center at (a_i, b_i) and dimensions H_i and W_i $(i = 1..m)$. The total wirelength for all terminal pairs (p_1, p_2) with p_1 anywhere in the $N \times M$ region (call this region B_0) and p_2 inside the obstacle B_i is found as (Fig. 2)

$$\bar{\ell}(B_0, B_i) = \int_0^N \int_{a_i - W_i/2}^{a_i + W_i/2} \int_0^M \int_{b_i - H_i/2}^{b_i + H_i/2} L_M(p_1, p_2) dy_2 dy_1 dx_2 dx_1, \quad (8)$$

with $L_M(p_1, p_2)$ the Manhattan distance between p_1 and p_2. The entire average redistribution wirelength can then be calculated by noting that it is given by the intrinsic wirelength of all terminal pairs in B_0, excluding those pairs for which at least one of the terminals is located inside an obstacle. Using the equivalence with sets, we want to enumerate over all pairs in $(B_0 \setminus (\cup_{i=1}^m B_i)) \times (B_0 \setminus (\cup_{i=1}^m B_i))$ which results in

$$\bar{L}_R = \frac{\bar{\ell}(B_0, B_0) - 2\sum_{i=1}^m \bar{\ell}(B_0, B_i) + \sum_{i=1}^m \sum_{j=1}^m \bar{\ell}(B_i, B_j)}{(NM - \sum_{i=1}^m W_i H_i)^2} \quad (9)$$

Similar equations exist for multi-terminal nets but lack the simple Manhattan distance expression for the wirelength.

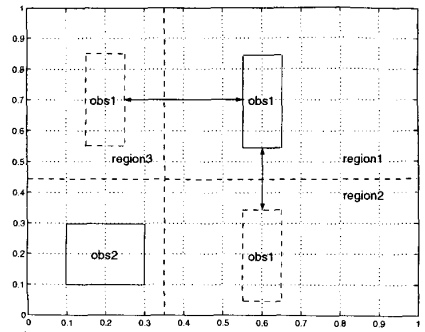

Fig. 8. Multiple obstacles with/without overlapping x- or y-span.

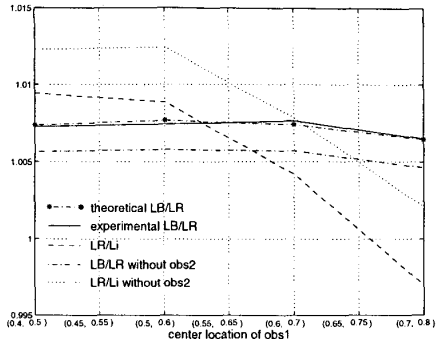

Fig. 9. Redistribution and blockage effects for region 1.

The blockage effect is much more difficult to calculate for m obstacles. However, if the m obstacles do not overlap in x- or y-spans then wires can only be blocked by a single obstacle at a time, and the average blockage can be found as the weighted sum

$$\bar{L}_b(n) = \frac{\sum_{i=1}^{m}(NM - W_iH_i)^2\,\bar{L}_{b,i}}{(NM - \sum_{i=1}^{m} W_iH_i)^2} \tag{10}$$

where $\bar{L}_{b,i}$ is given by Equation 6 for two-terminal nets or a more complicated expression for multi-terminal nets. We say that the blockage effect is *additive* (the denominator is taken care of by the redistribution effect) and we can treat the problem as a combination of single obstacle problems. However, in the general case, the assumption that x- and y-spans of blockages do not overlap does not hold.

B. Experimental observations

To study the effect of multiple obstacles and seperate the cases where the effects are additive we put two obstacles in a unit square and consider different cases where x- or y-spans overlap and where they do not overlap. Fig. 8 shows the experimental setup: obstacle `obs1` (dimensions 0.1×0.3) is moved within the unit square, while the other obstacle `obs2` (dimensions 0.2×0.2) has a fixed position. For movements of obstacle `obs1` in region 1 (location of center) there is no overlap; in regions 2 and 3 there is overlap.

The results of the experiments are shown in Fig. 9 for region 1 and in Fig. 10 for region 2. The first figure shows that (i) the blockage effect is additive and (ii) the theoretical equations under the assumption that blockage is additive match the experimental results. In Fig. 10 this is no longer true (the theoretical expression overestimates the blockage effect) which indicates we need lookup tables to truly assess the effects of multiple obstacles with overlapping x- or y-spans.

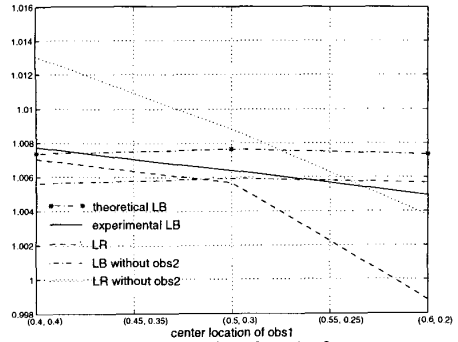

Fig. 10. Redistribution and blockage effects for region 2.

TABLE III
TOTAL EFFECT OF OBSTACLES ($\bar{L}_B/\bar{L}_i$) FOR TWO TERMINALS AS A FUNCTION OF TOTAL OBSTACLE AREA A AND NUMBER OF OBSTACLES m.

$m\backslash A$	0.1	0.2	0.3	0.4	0.5	0.6	0.7	0.8	0.9
1	1.0183	1.0283	1.0178	1.0427	1.0427	1.0427	1.0427	1.0427	1.0427
2	1.0184	1.0357	1.0432	1.0427	1.0378	1.0348	1.0342	1.0358	1.0333
4	1.0280	1.0639	1.0793	1.0783	1.0784	1.0736	1.0739	1.0730	1.0756
6	1.0459	1.0907	1.1210	1.1176	1.1204	1.1111	1.1119	1.1120	1.1140
8	1.0609	1.1180	1.1521	1.1458	1.1446	1.1429	1.1452	1.1423	1.1524
10	1.0709	1.1372	1.1776	1.1698	1.1716	1.1660	1.1696	1.1653	1.1663

We study the effect of a large number of obstacles by randomly generating a given number m of obstacles with a prescribed total obstacle area A.[8] Averaging out over a large number of experiments gives us a good indication for the average wirelength we can expect. Tables III and IV present the results (total wirelength over intrinsic length) for two- and three-terminal nets respectively. The total wirelength increases as the number of obstacles increases while the total obstacle area remains the same. This indicates that it is more beneficial to keep obstacles close together than to spread them over the entire surface! Another interesting observation is that wirelength seems, on average, not to depend on the obstacle area if it is large enough.

The main conclusions for multiple obstacles are:

Observation 9 *The redistribution effect for multiple obstacles can be found from Equation 9. Since it depends on correlations between obstacles, it is not additive in the general case.*

Observation 10 *The blockage effect is additive if there is no overlap in x- or y-span between all obstacle pairs. Otherwise, the calculation under the assumption that it is additive produces an overestimation of the blockage effect.*

Observation 11 *The total wirelength increases as the number of obstacles increases while the total obstacle area remains the same.*

[8]The algorithm is as follows: (1) read m and A; (2) generate $m-1$ random numbers between 0 and 1 to obtain each obstacle area; (3) generate the aspect ratio for each obstacle by using a normal distribution with mean 1; (4) obtain W and H for each obstacle; (5) for each obstacle, find a random position that fits in the unit square and has no overlap with other obstacles; (6) if no solution is found, repeat from step (2).

TABLE IV
TOTAL EFFECT OF OBSTACLES ($\bar{L}_B/\bar{L}_i$) FOR THREE-TERMINAL NETS AS A FUNCTION OF TOTAL OBSTACLE AREA A AND NUMBER OF OBSTACLES m.

$m\backslash A$	0.1	0.2	0.3	0.4	0.5	0.6	0.7	0.8	0.9
1	1.0463	1.1066	1.1553	1.2818	1.2818	1.2818	1.2818	1.2818	1.2818
2	1.0482	1.0953	1.1447	1.1556	1.1491	1.1272	1.1402	1.1390	1.1389
4	1.0893	1.1461	1.1883	1.2070	1.2011	1.2057	1.2114	1.1980	1.1957
6	1.1169	1.1911	1.2398	1.2491	1.2465	1.2631	1.2615	1.2406	1.2410
8	1.1557	1.2433	1.2796	1.2845	1.2737	1.2795	1.2790	1.2744	1.2875
10	1.2072	1.2800	1.3191	1.3256	1.3118	1.3158	1.3262	1.3001	1.3146

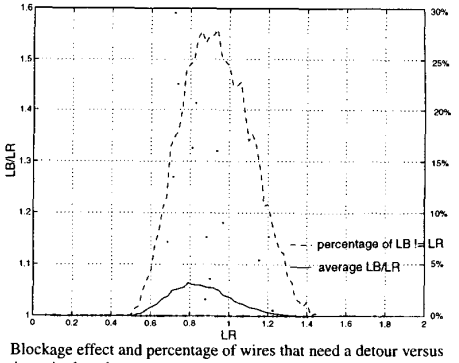

Fig. 11. Blockage effect and percentage of wires that need a detour versus redistribution wire length.

Observation 12 *For average block locations, the total wirelength does not depend on the obstacle area if it is large enough.*

IV. Applications to Wirelength Models

For SOC designs, large IP blocks have considerable influence on the routing length in the remainder of the design. Once the IP block locations are chosen, the redistribution effect on wirelength can be calculated as explained in Section III and is fixed. The actual wire locations will have to be decided taking the blockage effect into account. The tables we presented for blockage wirelengths can therefore also be used in combination with traditional wirelength estimators for guiding placement and routing.

Traditional wirelength estimators generally contain two main parts [5], a *site function* that enumerates [7] all possible shortest wire lengths (possible paths) between points in a grid[9] and a *probability distribution* that assigns to each path a probability of occurrence. The site function does not take detours because of obstacles into account. The tables provided by our experiments that relate blockage wirelength to redistribution wirelength can therefore be used to tune the site functions to the situation with obstacles.

Our technique is also able to relate the blockage effect to individual wires rather than to the average length. This is very useful for tuning results of wirelength estimators to the situation with obstacles. In Fig. 11, the blockage change is plotted as a function of redistribution wire length for a large number of individual wires. Also the percentage of wires that need a detour because of the blockage is shown. As can be expected, most very short wires are far from the obstacle and need no detour at all. The ratio of average blockage wirelength over redistribution wirelength thus is very close to 1. The same effect occurs for very long wires but for different reasons. Long wires have a lot of possibilities for routing along a shortest path and the probability that all of those intersect the obstacle is very small to non-existent. Medium-sized wires are most likely to "feel" the obstacle's presence. The figure shows that around 30% of those wires have to make a detour. For them, the blockage effect can be quite large, up to a 60% increase in wirelength.

To study the effect of blockages on wirelength predictors more closely, we are currently adopting the enumeration technique based on generating polynomials [7] which will allow us to augment current wirelength estimation techniques with our analysis of obstacle effects on an individual wire basis.

V. Conclusion

The inclusion of IP blocks in SOC design potentially has large effects on the wirelengths in the rest of the design. In this paper, we have studied both the effect of redistributing net terminals outside of obstacle regions and the detours that wires have to make due to the obstacles. Several parameters influence the effects: the aspect ratio of the design, the dimensions and location of the obstacle(s), the number of obstacles and the number of net terminals. We derived analytical expressions for the simple yet important case of a single obstacle and two-terminal nets. More complex situations with multiple obstacles and multi-terminal nets require an experimental approach.

Our experiments lead to 12 observations that can be used as guidelines for the inclusion of obstacle effects in wirelength models. The tables that can be filled with information from our technique[10] can be used by floorplanning tools to decide on the "ideal" obstacle location to reduce average wirelength. Our analysis of the blockage effect on individual wirelengths also provides a way of tuning individual wirelength estimations, and overall our work can potentially improve the accuracy of placement and routing tools.

Further research on this topic is needed to concentrate on such issues as the following.

1. For large obstacles, a lot of detours follow the obstacle boundary but these wires are not infinitely thin (as we implicitly assumed). The real detour will hence be longer than the one we consider in this paper.
2. We plan to also study in detail the effect of many very small obstacles (this could be useful for assessing the effect of vias on routing).
3. Our analysis can be further extended to include alternative non-uniform pin distributions to adapt to different circuit topologies.

[9] This enumeration thus results in the redistribution wire length for given obstacle locations.

[10] Only a few examples could be shown in this draft due to space limits.

References

[1] B. S. Landman and R. L. Russo, "On a Pin versus Block Relationship for Partitions of Logic Graphs", *IEEE Trans. on Computer*, C-20, 1971, pp. 1469-1479.

[2] W. E. Donath, "Placement and Average Interconnection Lengths of Computer Logic", *IEEE Trans. on Circuits and Systems*, CAS-26(4), 1979, pp. 272-277.

[3] J. A. Davis, V. K. De and J. D. Meindl, "A Stochastic Wire- Length Distribution for Gigascale Integration(GSI)-part 1: Derivation and Validation", *IEEE Trans. on Electron Dev.*, 45, 1998, pp. 580-589.

[4] D. Stroobandt, "Tutorial: A Priori Wire Length Estimations Based on Rent's Rule", *Workshop on System-Level Interconnect Prediction (SLIP)*, 1999, pp. 3-50.

[5] P. Christie and D. Stroobandt, "The Interpretation and Application of Rent's Rule", *IEEE Trans. on VLSI Systems, Special Issue on System-Level Interconnect Prediction*, 2000.

[6] D. Stroobandt and J. Van Campenhout, "Accurate Interconnection Length Estimations for Predictions Early in the Design Cycle,", *VLSI Design, Special Issue on Physical Design in Deep Submicron*, 10(1), 1999, pp. 1-20.

[7] D. Stroobandt and H. V. Marck, "Efficient Representation of Interconnection Length Distributions Using Generating Polynomials", ACM Workshop on *System-Level Interconnect Prediction (SLIP)*, 2000, pp. 99-105.

[8] A. E. Caldwell, A. B. Kahng, S. Mantik, I. L. Markov and Alex Zelikovsky, "On Wirelength Estimations for Row-Based Placement", *International Symposium on Physical Design(ISPD)*, 1998, pp.4-11.

[9] C. E. Cheng, "RISA: Accurate and Efficient Placement Routability Modeling", *Proceedings of 1994 IEEE International Conference on Computer-Aided Design*, 1994, p.690-695.

[10] L. Scheffer and E. Nequist, "Why Interconnect Prediction Doesn't Work," *Proc. ACM Workshop on System-Level Interconnect Prediction*, 2000, p.139-144.

[11] Technical Report, April 2000. Anonymous for review process. http://www.geocities.com/aspdac2001.

[12] L. Kou, G. Markowsky and L. Berman, "A Fast Algorithm for Steiner Trees," *Acta Informatica*, 15(2), 1981, pp. 141-145.